J. Eng. Technol. Sci., Vol. 53, No. 5, 2021, 210505

Improved Modified Symbiosis Organisms Search (IMSOS): A New and Adaptive Approach for Determining Model Parameters from Geoelectrical Data

Sungkono[1] & Hendra Grandis[2]

[1]Departement of Physics, Institut Teknologi Sepuluh Nopember,
Jalan Arief Rachman Hakim, Surabaya 60111, Indonesia
[2]Faculty of Mining and Petroleum Engineering, Institut Teknologi Bandung,
Jalan Ganesha 10, Bandung 40132, Indonesia
E-mail: hening_1@physics.its.ac.id

Highlights:

- Improved Modified Symbiosis Organisms Search (IMSOS) is proposed to improve the standard Modified Symbiosis Organisms Search (MSOS) algorithm.
- IMSOS was tested on the inversion of geoelectrical data (self-potential and vertical electrical sounding measurements), both synthetic and field data.
- IMSOS accurately determined the model parameters and model uncertainty.
- Like SOS and MSOS, IMSOS is also tuning parameter free.

Abstract. Symbiotic Organisms Search (SOS) is a global optimization algorithm inspired by the natural synergy between the organisms in an ecosystem. The interactive behavior among organisms in nature simulated in SOS consists of mutualism, commensalism, and parasitism strategies to find the global optimum solution in the search space. The SOS algorithm does not require a tuning parameter, which is usually used to balance explorative and exploitative search by providing posterior sampling of the model parameters. This paper proposes an improvement of the Modified SOS (MSOS) algorithm, called IMSOS, to enhance exploitation along with exploration strategies via a modified parasitism vector. This improves the search efficiency in finding the global minimum of two multimodal testing functions. Furthermore, the algorithm is proposed for solving inversion problems in geophysics. The performance of IMSOS was tested on the inversion of synthetic and field data sets from self-potential (SP) and vertical electrical sounding (VES) measurements. The IMSOS results were comparable to those of other global optimization algorithms, including the Particle Swarm Optimization, the Differential Evolution and the Black Holes Algorithms. IMSOS accurately determined the model parameters and their uncertainties. It can be adapted and can potentially be used to solve the inversion of other geophysical data as well.

Keywords: *free tuning parameter; geoelectrical data; model parameter; inverse problem; uncertainty analysis.*

Received December 3rd, 2020, Revised May 10th, 2021, Accepted for publication June 11th, 2021.
Copyright ©2021 Published by ITB Institute for Research and Community Services, ISSN: 2337-5779,
DOI: 10.5614/j.eng.technol.sci.2021.53.5.5

1 Introduction

Geoelectrical data (for example from self-potential and vertical electrical sounding measurements) can be used to determine relevant subsurface parameters. In order to determine these parameters, data inversion is required. Data inversion is not only done to optimize misfit between observed and calculated data but also to evaluate the posterior distribution of models (PDM) and quantify the model uncertainties. The latter represents, at least in part, the non-uniqueness of the inverse problem solution. Causes of a non-unique solution in inversion results include noise contained in the measured data, bandwidth limitations, physical assumptions (e.g. isotropy, anisotropy, homogeneity, etc.), and numerical approximations for forward mathematical modeling [1-4].

Posterior sampling, generally performed by applying the Monte Carlo (MC) technique, is done to derive the uncertainties of the inversion modeling solution. MC is computationally expensive since the posterior sampling necessitates calculation of the likelihood function [5]. However, some meta-heuristic algorithms (MHAs), including the Genetic Algorithm (GA) [6], the Particle Swarm Optimization (PSO) [7], the Differential Evolution (DE) [8], the Black Holes Algorithm (BHA) [9], the Flower Pollination Algorithm (FPA) [10], etc. provide posterior sampling of model parameters with the capacity to trade off between exploration and exploitation of the search space.

The most notable advantages of MHAs are their independence from the initial model and avoidance of gradient-based calculation to find the global optimum solution. However, the results of some MHAs depend on the controlling parameters. For example, 1) GA requires mutation and crossover probabilities; 2) PSO requires inertia weight, cognitive and social parameters; 3) FPA requires switching probability; 4) DE involves a weighting factor and crossover probability, etc. Furthermore, some MHAs require parameter tuning to balance the exploration and exploitation capacities of the algorithm. Improper tuning of the MHA parameters may lead to a non-optimum solution and may increase the computational time required for inversion. Several tuning parameter free MHAs have been proposed, including the Black Hole Algorithm [9,11], the Symbiosis Organisms Search (SOS) [12], the Ions Motion algorithm [13], the Dragonfly algorithm [14], the Adaptive Differential Evolution [15], the Marine Predatory algorithm [16], etc. Sometimes, the weak exploitation capability of tuning parameter free MHAs leads to very slow convergence because of stagnation at local optima.

A simple, yet powerful and relatively fast convergence MHA that does not need parameter tuning is SOS, proposed by Cheng & Prayogo [12]. The algorithm simulates symbiotic interaction strategies that organisms use to survive in their

ecosystem. The SOS algorithm was successfully applied to solve non-linear and multimodal problems, for example in structural optimization [12,17,18], power plants and system optimization [19], and antenna design [20]. In this paper, an improvement of the previously modified SOS algorithm for the inversion of geophysical data is proposed by providing posterior sampling of the model parameters. Noisy synthetic and field data from self-potential (SP) and vertical electrical sounding (VES) measurements were used to test the performance of the proposed IMSOS algorithm in the inversion process. All inversion estimation problems considered here are highly non-linear and have non-unique solutions [9,21].

2 Symbiosis Organism Search Algorithm

Symbiosis is the interaction or relationship between two different organisms in a natural ecosystem. The SOS algorithm was inspired by symbiosis mechanisms and contains mutualism, commensalism and parasitism phases [12]. Mutualism symbiosis describes the interaction of two organisms where both of them benefit from this interaction. Commensalism symbiosis denotes interaction where one of the organisms involved obtains the benefits from another organism, which is not affected by the relationship. Finally, parasitism symbiosis is the interaction between two organisms where one organism survives by harming the other organism.

2.1 Mutualism Phase

For processing in the mutualism phase, for each organism X_i, an organism X_j is selected randomly from the ecosystem, where $X_i \neq X_j$. The interaction between X_i and X_j is to increase the mutual survival advantages within the ecosystem by creation of new organisms as follows:

$$X_{inew} = X_i + rand(0,1) \times (X_{best} - X_{mutual} \times BF_1) \tag{1}$$

$$X_{jnew} = X_j + rand(0,1) \times (X_{best} - X_{mutual} \times BF_2) \tag{2}$$

where X_{best} denotes the organism with the best objective function value or fitness and $rand(0,1)$ is a vector of random numbers uniformly distributed between 0 and 1. Furthermore, BF_1 and BF_2 reflect the benefit factors for each organism with respect to their interaction represented by X_{mutual}, as determined by

$$X_{mutual} = (X_i + X_j)/2 \tag{3}$$

The benefit factors in Eqs. (1) and (2) are stochastically chosen as either 1 or 2 by using

$$BF_1 = 1 + round[rand(0,1)] \tag{4}$$

$$BF_2 = 1 + round[rand(0,1)] \tag{5}$$

The new candidates for solutions X_{inew} and X_{jnew} replace X_i and X_j, respectively, if their fitness is better than that of the organisms before interaction. Otherwise, X_i and X_j as the initial organisms are retained. In this case, organisms in the ecosystem represent models in the model space, where the indices *i* and *j* refer to models in the population.

Eqs. (1) and (2) show that an organism can partially or fully benefit from the interaction process. The level of benefit from the interaction is expressed in the value of the benefit factor. A small benefit factor is associated with a small step in the algorithm search, including the exploitation capacity, which may decrease the convergence speed of the algorithm. Conversely, a large benefit factor may be beneficial for the exploration property of the algorithm and for the convergence speed. Thus, the exploitation and exploration capacities of the mutualism phase depend on the benefit factor. Consequently, in order to obtain a good balance between the exploitation and exploration of the algorithm some authors have proposed an adaptive method to determine the benefit factor [17,18] to replace Eqs. (4) and/or (5). In this study, following Kumar, *et al.* [17], the adaptive benefit factor was determined based on an objective function that varies throughout the iteration process, i.e.

$$ABF = \begin{cases} f(X_i)/f(X_{best}) & \text{if } f(X_{best}) \neq 0 \\ 1 + round[rand(0,1)] & \text{if } f(X_{best}) = 0 \end{cases} \tag{6}$$

Furthermore, benefit factor BF_1 in Eq. (1) is determined as follows:

$$BF_1 = \begin{cases} 1 & \text{if } ABF < 1 \\ 2 & \text{if } ABF > 1 \\ ABF & \text{otherwise} \end{cases} \tag{7}$$

2.2 Commensalism Phase

In the commensalism phase, an organism X_i interacts with another organism X_j chosen randomly from the ecosystem, where $X_i \neq X_j$. The interaction is such that X_i increases its opportunity to survive by taking advantage from X_j without affecting X_j. A new candidate for the solution in the commensalism phase is created by

$$X_{inew} = X_i + rand(-1,1) \times (X_{best} - X_j) \tag{8}$$

where *rand*(-1,1) is a vector of random numbers uniformly distributed between -1 and 1. The comparison of the fitness values of X_i and X_{inew} determines which organism will survive for the next generation.

2.3 Parasitism Phase

In the parasitism phase, the interaction between organisms is analogous to the interaction between Plasmodium parasites, Anopheles mosquitos and humans. The human host is harmed, while the Anopheles mosquito as parasite carrier is left unharmed and the Plasmodium parasite obtains a benefit, because it can reproduce in the human body. Parasites in humans are generally not only of one kind and different parasites can interact among each other. In such cases, for a given organism X_i, an artificial parasite vector is created based on other organisms X_j, X_k and X_l, randomly selected from the ecosystem serving as hosts to $X_{parasite}$. We use a slightly modified formula from Kumar, *et al.* [17] for $X_{parasite}$, as follows:

$$X_{parasite} = \begin{cases} X_i & \text{if } rand(0,1) \geq 0.5 \\ X_j + rand(0,1)(X_k - X_l) & \text{otherwise} \end{cases} \quad (9)$$

Furthermore, the parasite vector will try to replace X_i in the ecosystem using greedy selection, i.e. by comparing their fitness. Eq. (9) is a mutation strategy like in other MHAs, which is to avoid premature convergence and to explore different regions of the search space. In addition, Eq. (9) requires three randomly selected models from the population, such that the computational time may slightly increase compared to the original modified SOS (MSOS).

2.4 SOS Properties

The success rate of MHAs in solving problems depends on the exploitation and exploration capabilities of the algorithm. Exploitation represents local search capability around a potential solution, leading to faster convergence, while exploration implies that the algorithm is able to sample different parts of the search space to find the global optimum, which is usually associated with slow convergence. Ideally, MHAs have to converge relatively fast and simultaneously find an accurate solution associated with the global optimum. This condition will be fulfilled when the MHA has a good balance between its exploration and exploitation capabilities.

The exploitation property of the SOS algorithm is correlated with the mutualism and commensalism phases, while the exploration capability is associated with the mutualism and parasitism phases [12,22]. More specifically, the exploitation capability of SOS is related to factors such as: 1) partial benefit of the organism

from the interaction in the mutualism phase related to a small benefit value; 2) common interaction in the commensalism phase, which is also used in other global optimization algorithms, including DE and GA; 3) the use of the best solution as reference point in the commensalism phase to exploit promising regions [12,17,22]. Meanwhile, the exploration capability of SOS is related to factors such as: 1) a large benefit value in the mutualism phase, which induces the organism to fully benefit from the interaction, thus reducing exploitation; 2) a mutation-like operator used in the parasitism phase for preventing premature convergence and maintaining diversity [17,22].

Strategies that may be used to balance the exploration and exploitation capabilities of the SOS algorithm include: 1) using an adaptive benefit factor in the mutualism phase [17]; 2) using the original SOS algorithm for exploitation in the commensalism phase [23], 3) using a mutation strategy in the parasitism phase [17]. Furthermore, greedy selection is applied in all phases to choose organisms that can survive in the ecosystem. This approach is applied by comparing the fitness of the new organism to the pre-interaction organisms.

3 Forward Modeling

Forward modeling describes the estimation of theoretical data for the model parameters, **m**. Forward modeling is denoted by $F(\mathbf{m})$. Formulas for some forward modeling calculations used in this paper are presented briefly for completeness in the following sections.

3.1 Self-Potential (SP)

For an idealized body (e.g. sphere, horizontal cylinder and vertical cylinder), the SP anomaly at a point x_i can be expressed as follows [24,25]:

$$v(x_i) = K \frac{(x_i - D)\cos(\theta) + h\sin(\theta)}{((x_i - D)^2 + h^2)^q} \tag{10}$$

where K and θ are the polarization and the polarization angle, respectively, and h and D denote the depth and position (relative to the coordinate origin) of the anomalous source's center, respectively, while q represents the shape factor. The shape factor is 0.5, 1.0 and 1.5 for a vertical cylinder, a horizontal cylinder and a sphere, respectively. Hence, $F(\mathbf{m}) = v(x_i)$, where **m** contains K, θ, h, D and q.

3.2 Vertical Electrical Sounding (VES)

The VES response of a layered earth or 1D model is apparent resistivity ρ_a, which can be determined from the convolution formula as follows [21,26]:

$$\rho_a = \sum_{k=k\min}^{k\max} T_1(\lambda_k)\, f_k \tag{11}$$

where f_k are linear filter coefficients as a function of the measurement configuration used. $T(\lambda)$ is the resistivity transform function, which can be calculated by using Pekeris' recursion formula as follows [21, 26]:

$$T_i(\lambda) = \frac{T_{i+1}(\lambda) + \rho_i \tanh(\lambda h_i)}{1 + T_{i+1}(\lambda) \tanh(\lambda h_i)/\rho_i} \qquad i = n\text{-}1, n\text{-}2, \ldots, 1 \tag{12}$$

For an n-layered model $T_n = \rho_n$, hence $T_1(\lambda)$ is the resistivity transform at the surface, while ρ_i and h_i are the resistivity and the thickness of the i-th layer, respectively. Therefore, in the VES method $F(\mathbf{m}) = \rho_a$, $\mathbf{m}$ contains ρ_i and h_i, i = 1, 2, …, n, where n is the total number of layers in the 1D model.

4 Inversion

Inversion is a process to determine model parameters from observed data by fitting calculated data $F(\mathbf{m})$ to observed data $\mathbf{d}$. For a non-linear relationship between the model and the data, expressed in forward modeling function $F(\mathbf{m})$, most inversions obtain a solution by linearization and updating the initial model iteratively so that it converges to the best model [4].

The inversion process using a global optimization algorithm is generally geared to minimize an objective function. In order to invert SP data, the objective function Obj_{SP} can be defined as follows [25]:

$$Obj_{SP} = \frac{2 \| d_i - F_i(\mathbf{m}) \|}{\| d_i - F_i(\mathbf{m}) \| + \| d_i + F_i(\mathbf{m}) \|} \tag{13}$$

where d_i and $F_i(\mathbf{m})$ describe the i-th element of the observed and the calculated SP data, respectively, while $\| \cdot \|$ denotes the vector magnitude operator or sum over the absolute values of the vectors' elements. Using the same notation, the objective function for VES is expressed as follows:

$$Obj_{VES} = \frac{\| \log(d_i / F_i(\mathbf{m})) \|}{\| \log(d_i) \|} \times 100 \tag{14}$$

Solutions to geophysical inverse problems are generally not unique due to the presence of noise and the inherent theoretical relationship between the observed parameters or data and the model parameters. Consequently, many models with different combination of parameters can be considered optimum solutions, i.e. the predicted data fit the observed data.

The use of MHAs is a good option for solving inversion problems in order to provide a set of equivalent models since they have the exploration capacity to find solutions in the search space. In such cases, MHAs provide an effective and efficient sampling mechanism, which can lead not only to the best model but also to a set of models fulfilling certain criteria of optimality, i.e. low misfit. For example, inversion that uses the Black Holes Algorithm and PSO variants [7,9,11] may result in a large number of models M_{tol} that fit the observed data **d** within misfit tolerance *tol* as follows [2]:

$$\mathbf{m} \in M_{tol} : Obj(\mathbf{m}) \leq tol \tag{15}$$

The only problem with the exploration property of MHAs is that they are more time-consuming in obtaining convergence. Therefore, in order to obtain a set of good models, MHAs should balance their exploitation and exploration capabilities, where SOS is one of the MHAs that have that ability without tuning parameter, as described in Section 2.4.

5 Algorithm Testing

The performance and reliability of Improved Modified SOS (IMSOS) and Modified SOS (MSOS) [17] were compared by evaluation of the well-known Ackley and Griewank functions. The upper and lower bounds were set to [-600, 600] and [-32, 32] for the Griewank and the Ackley testing function, respectively. IMSOS and MSOS were tested in solving 30 dimensions of both functions, which are multimodal functions that are generally used to evaluate unconstrained algorithm performance, as in inversion problems. The tests were run for 5 times to demonstrate the consistency and performance of both algorithms.

The results showed that IMSOS performed better than MSOS in finding the global minimum (Figures 1(a) and 1(b)) for both the Ackley and the Griewank testing function, with both algorithms having comparable explorative capabilities (Figures 1(c) and 1(d)). Therefore, IMSOS improved its exploitation capability while maintaining its exploration capability (diversity of the population).

6 Application to Synthetic Data

The IMSOS algorithm was applied to invert synthetic SP and VES data using the parameters in Tables 1 and 2, respectively. In inversion, the model parameters that represent the organism are contained in *X*, while the mutualism, commensalism and parasitism phases are applied to search for optimum models and to construct the posterior distribution of models (PDM), which requires number of function evaluations (NFE). Furthermore, the stopping criteria for all

algorithms is the maximum number of function evaluations, FE_{max}, which was set to 80000 and 2000 evaluations for SP and VES inversion, respectively.

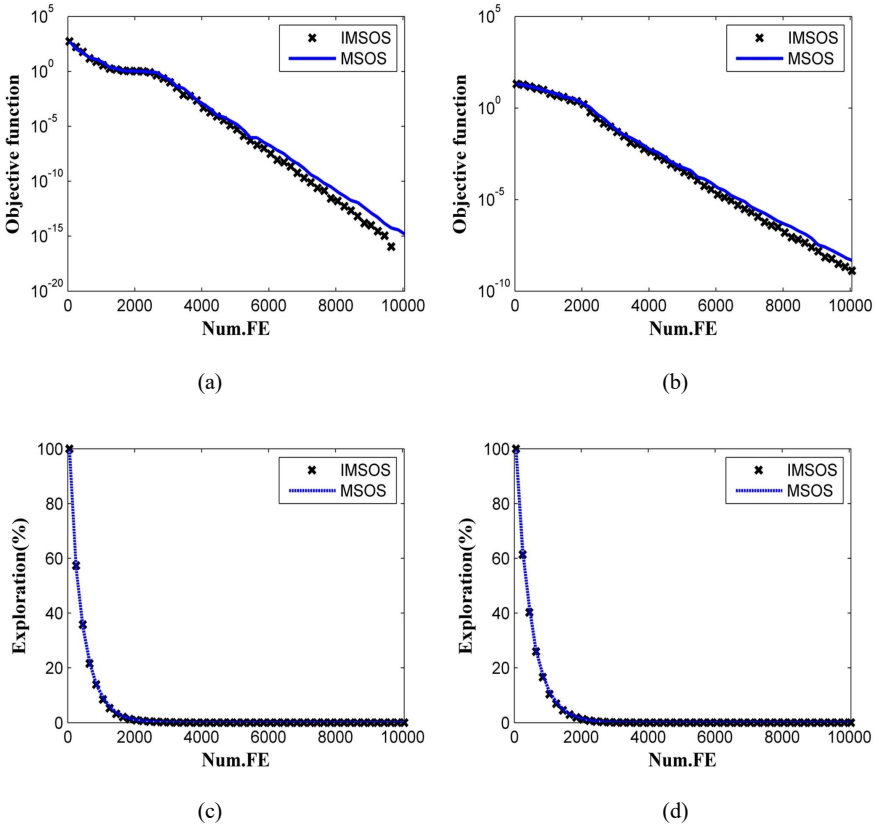

Figure 1 Convergence curves for the Griewank function (a) and the Ackley function (b), and the explorative capabilities for the Griewank function (c) and the Ackley function (d).

6.1 Self-Potential Data

The synthetic SP data associated with two-body anomalies were generated by using Eq. (10) with 5% Gaussian noise added. Table 1 presents the synthetic model parameters, the parameter model bounds for the search spaces and the inversion results from the IMSOS algorithm. Recently, MHAs have succeeded in recovering the model parameters of multiple SP anomaly sources, including BHA [9], PSO [25], the Genetic Prices Algorithm (GPA) [27], Very Fast Simulated Annealing (VFSA) [28], the Flower Pollination Algorithm (FPA) [10] and the

Whale Optimization Algorithm (WOA) [29]. GPA and VFSA need many more forward modeling evaluations for global optimization compared to the other algorithms [9,10,25,29]. We compared inversion using IMSOS to PSO [25] and BHA [9], where both IMSOS and BHA algorithms were successful in inverting SP data containing multi-body anomalies. BHA is tuning parameter free, while the PSO inversion parameters were set as in by Monteiro-Santos [25].

Table 1 True parameters, search space, inversion results and their uncertainties (median ± iqr) from BHA and SOS for synthetic SP data.

Parameters	K	D (m)	h (m)	θ (^{O})	q
True anomaly 1	1000	-100	7	40	1.5
True anomaly 2	-400	30	30	60	1
Ranges of anomaly 1	0 to 2000	-150 to -50	0 - 100	0 - 180	0.1 - 1.8
Ranges of anomaly 2	-700 to 700	-50 to 150	0 -100	0 - 180	0.1 - 1.8
Anomaly 1 (IMSOS)	926.56±163.28	-99.80±0.54	6.97±0.63	31.42±4.55	1.48±0.03
Anomaly 2 (IMSOS)	-182.65±20.22	31.46±1.05	25.94±1.00	65.19±1.77	0.90±0.01
Anomaly 1 (BHA)	820.41±71.78	-99.75±0.45	8.57±3.64	35.30±6.16	1.41±0.06
Anomaly 2 (BHA)	-275.21±33.14	31.69±2.70	29.63±1.58	64.49±4.74	0.96±0.01

Figure 2(a) shows that the SP data fittings (median of the PDM) from IMSOS and BHA were better than from PSO, which can also be seen from the best objective function curves (Figure 2(b)). The theoretical response of the median model from PDM tended to fit the observed data equally well [9]. In addition, Figure 2c illustrates that BHA had the best explorative capability. Nevertheless, the method also had good balance between its exploration and exploitation capabilities, with a large interquartile (iqr) and the lowest best objective function. The IMSOS algorithm also has balanced capacities, while PSO could not find the global minimum. Thus, BHA and IMSOS outperformed the PSO algorithm, probably due to the tuning parameter of the algorithm not being appropriately set. As a consequence, the algorithm was likely to get trapped in a local minimum.

Figure 3 represents the PDM of the model parameters constructed by IMSOS using tolerance 0.3 for the objective function. The statistics of the PDM are presented in Table 1, compared to the BHA inversion results. In this case, the PSO inversion results did not lead to a PDM, because none of the particles from all iterations met Eq. (13), as can be seen in Figure 1(b). Table 1 also shows that the IMSOS results were comparable with those from BHA, while PSO could not resolve the problem well, especially for anomaly 1. Furthermore, Figure 3 shows that the medians of the PDM from IMSOS were close to the true model parameters. This means that IMSOS has a good balance between exploration and exploitation capabilities in SP data inversion.

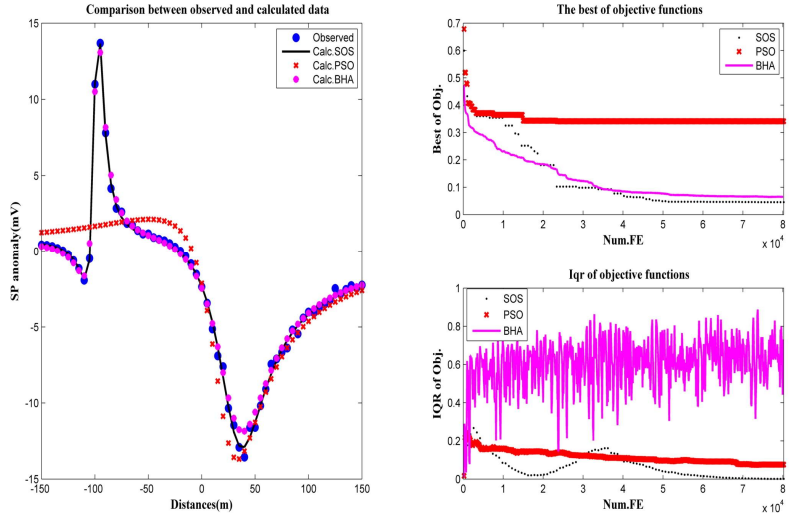

Figure 2 Comparison between the synthetic and the calculated SP data from the PSO, BHA and SOS median models, and the properties from PSO, BHA and SOS for the synthetic SP data, including the best and interquartile of the objective function with number of function evaluations (NFE).

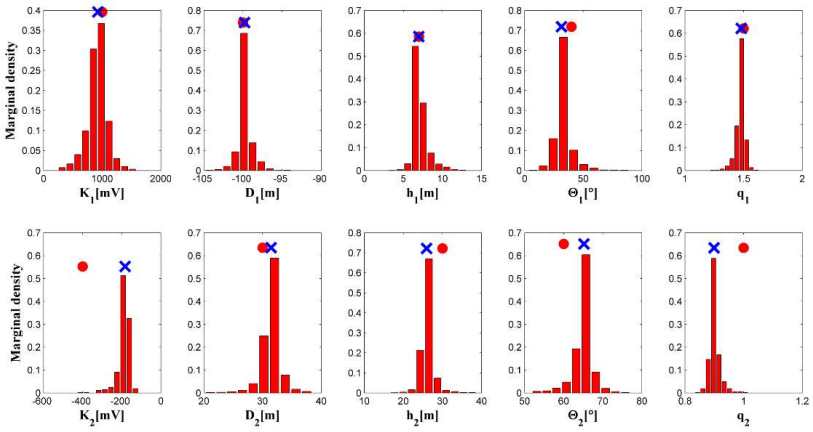

Figure 3 Histogram provided by IMSOS from the synthetic SP data, where crosses indicate the median from the model samples, while dots indicate the true model parameters.

6.2 Resistivity Data

VES synthetic data with a Schlumberger array for a three-layered earth model was calculated by using Eq. (11) with 5% Gaussian noise added to the synthetic apparent resistivity data to simulate noisy field data. Table 2 shows the true model parameters and the upper and lower bounds of the search space for inversion with DE and IMSOS. The DE parameters and strategy for VES data inversion were based on Balkaya [8].

Table 2 true parameters, search space, and inversions results from DE and IMSOS for synthetic VES data.

Parameters	True Model	Search Space	DE	IMSOS
h1 (m)	2	0.5 - 10	2.03±00	2.03±0.00
h2 (m)	25	5 - 50	22.44±0.01	22.44±0.00
ρ1 (Ωm)	2500	500 - 10000	2462.41±0.24	2462.41±0.09
ρ2 (Ωm)	100	10 - 1000	98.86±0.01	98.86±0.01
ρ3 (Ωm)	300	10 - 3000	288.22±0.04	288.22±0.00

Figure 4 shows the convergence and dispersion curves, indicating that IMSOS and DE have the same exploration and exploitation capabilities. In order to construct a PDM, a threshold of 1.2 was set for the objective function. Figure 5 is the histogram of the PDM for IMSOS, with the true model parameters and the median of the PDM represented by red dots and green crosses, respectively. Table 2 and Figure 6 contain a comparison of the results in terms of PDM statistics for DE and IMSOS, which show that the IMSOS results were comparable to the DE results and both results were close to the true model parameters from the VES synthetic data. Furthermore, Figure 6 also shows a good fit between the observed (or synthetic) and the calculated VES data using DE and IMSOS from the best model in terms of RMS error between observed and calculated data.

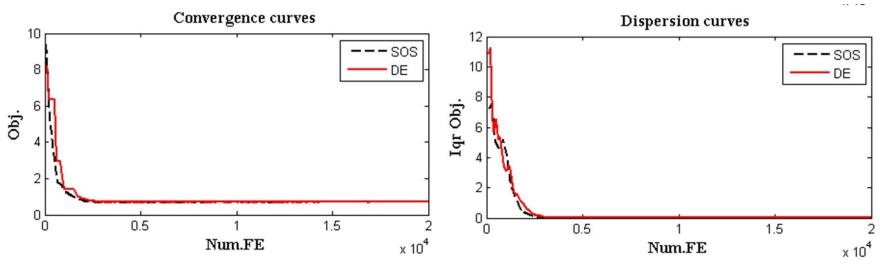

Figure 4 Comparison of IMSOS and DE in terms of the best objective function with NFE (left) and interquartile objective function with NFE (right).

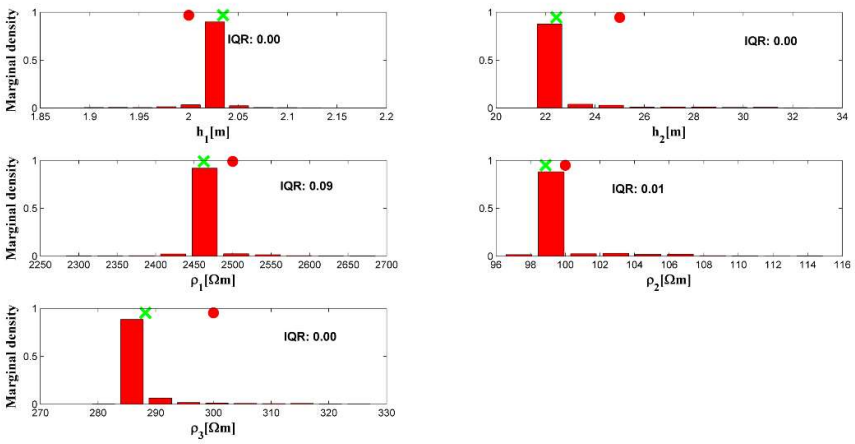

Figure 5 Histogram of PDM from synthetic VES data inversion using IMSOS, where crosses indicate the median model samples, while dots indicate the true model.

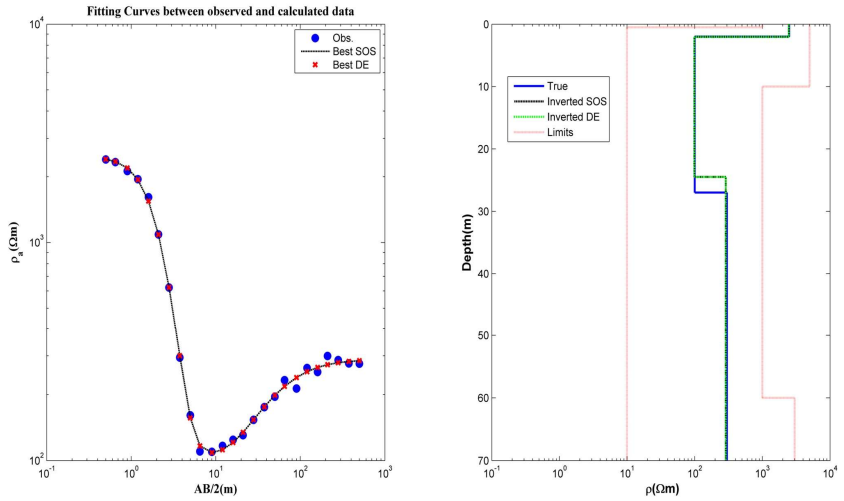

Figure 6 (a) Comparison of synthetic VES data (solid dots) and calculated response of the best models from IMSOS (dashed lines) and DE (crosses) (left), inverse 1D model from the best model of IMSOS (dashed lines) and DE (dash-dot) compared to the synthetic model (full line). The interval of the search space is shown as an envelope of all lines (right).

7 Application to Field Data

7.1 Self-Potential Data

Field SP data were measured at P79-P83, in the embankment area of the LUSI mudflow, Sidoarjo, East Java, Indonesia. As detailed in previous works [9,30,31], the embankment is unstable and has collapsed several times. Sungkono & Warnana [9] interpreted the SP data using BHA as four horizontal cylindrical structures. Some structures may be correlated with piping or seepage in the embankment. We also assumed that the SP data can be associated with four anomalous sources. The limits of the search spaces were similar with those used in BHA inversion, while FE_{max} was set to 300,000 evaluations. Figure 7 shows a comparison of the SP data inversion results using IMSOS and BHA, while Table 3 lists the numerical values. Figure 7b and Figure 7c indicate that BHA is more explorative than IMSOS. However, IMSOS had explorative capability up to 70,100 of NFE and a lower final objective function.

The uncertainty of the model parameters from inversion is constructed by using Eq. (15). Table 3 indicates that the uncertainty of the model parameters of IMSOS was in good agreement with the BHA results, especially concerning the factors of distance, depth and shape. In addition, the IMSOS results also showed that the shape of the models was around 1, which is associated with a horizontal cylinder ($q \approx 1$). These anomalies are interpreted as horizontal fractures that are affected by deformation in this area [9,30,31].

Table 3 Inversion parameters (search space) and results (model parameters) and their uncertainties using IMSOS compared to BHA [9] for field SP data.

Parameter	Anomaly	K	D	h	θ	q
Parameter range	Body 1	-700 to 0	0 - 75	0 - 80	0 - 180	0.3 - 1.8
	Body 2	-700 to 0	75 - 110	0 - 80	0 - 180	0.3 - 1.8
	Body 3	0 to 700	150 - 215	0 - 80	0 - 180	0.3 - 1.8
	Body 4	-700 to 0	200 - 300	0 - 80	0 - 180	0.3 - 1.8
BHA [9]	Body 1	-412.99±4.47	46.46±0.60	16.16±0.35	104.07±1.85	1.06±0.00
	Body 2	-386.59±11.10	99.69±0.39	15.76±0.59	85.88±2.88	1.14±0.01
	Body 3	480.60±27.95	154.93±0.76	25.61±0.36	140.23±2.02	1.01±0.01
	Body 4	-563.42±10.49	268.04±2.10	18.93±0.43	103.75±6.47	1.17±0.19
IMSOS	Body 1	-303.83±49.88	40.99±1.20	15.01±2.25	74.26±5.11	1.17±0.19
	Body 2	-493.38±48.24	89.57±13.29	13.07±7.42	14.99±62.90	1.20±0.14
	Body 3	634.83±22.73	140.22±2.65	17.93±0.79	91.99±8.70	1.03±0.03
	Body 4	-574.72±17.18	279.11±2.56	21.69±0.59	136.62±6.72	1.06±0.01

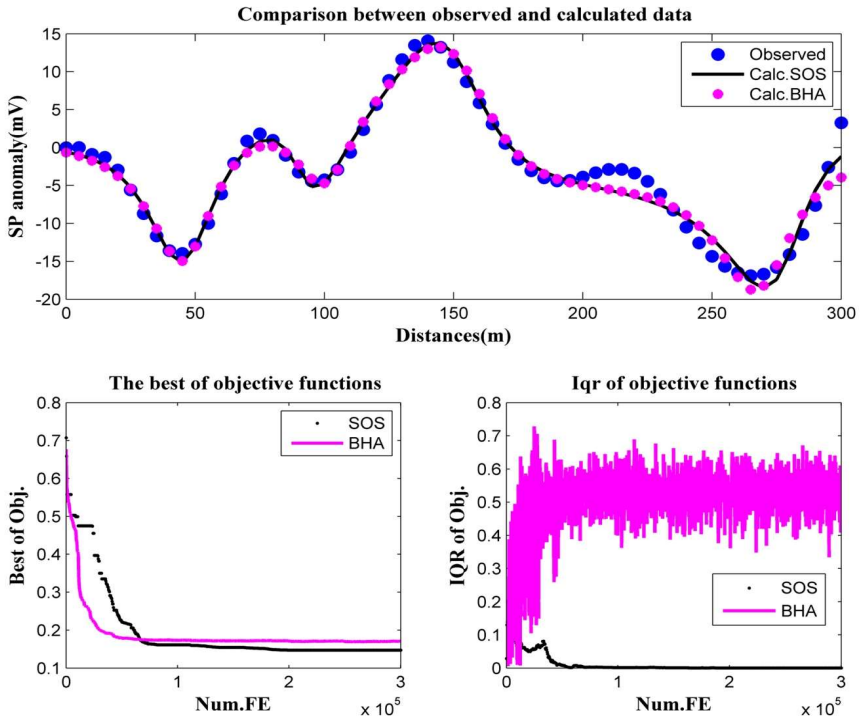

Figure 7 Inversion results using IMSOS and BHA of SP data from the LUSI embankment: observed and calculated SP data, convergence of the best objective functions and dispersion curves represented by the iqr of the objective functions.

7.2 Resistivity Data

Field VES data were also taken from P79-P83 at the LUSI embankment. The materials used to construct the embankment consist mainly of alluvium (clay, silt and sand) [32]. The thickness of the embankment area varied from 10 to 15 meter and is affected by water leakage. The VES data were measured by using a Schlumberger configuration for determining the thickness of the embankment. From Figure 8 it can be seen that IMSOS is slightly more explorative than DE for VES data inversion. In this case, FE_{max} was set to 20,000.

Using a tolerance of 3 from the convergence curve, the results from IMSOS were used to construct a PDM (Figure 9). The calculated VES data from the inverse models using IMSOS and DE showed a good match with the field data (Figure 10). Table 4 shows the median of the model parameters and their uncertainties are shown as bounds in the search space. Additionally, the result indicates that

the thickness of the embankment was around 11.88 ± 0.11 meter, by assuming that the embankment has higher resistivity compared to its base (clay) [31]. The result for embankment thickness was relatively close to the embankment design of LUSI, i.e. 11 meter [33]; the embankment has been repaired after failure in 2008.

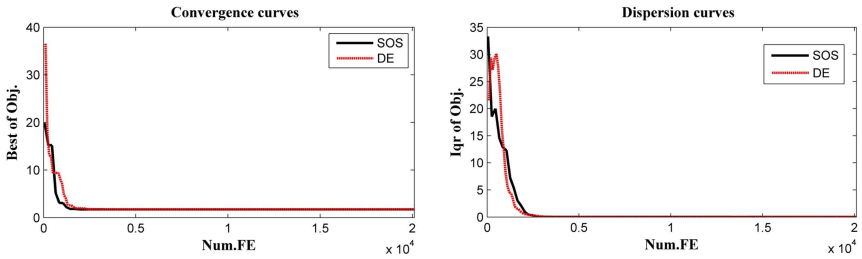

Figure 8 Convergence and dispersion curves from inversion of field VES data by using the IMSOS and DE algorithms.

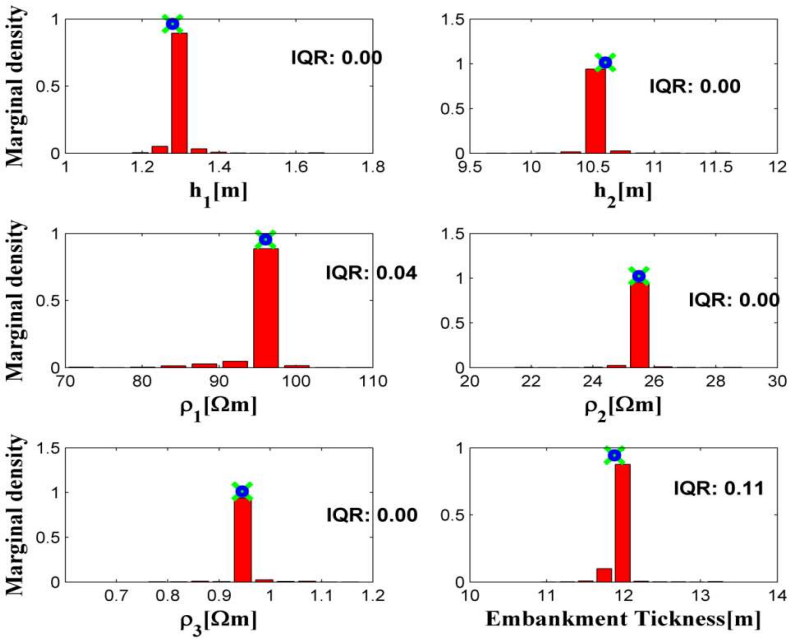

Figure 9 Histogram for model parameter estimates from IMSOS inversion of field VES data. The embankment thickness was determined by the sum of the thickness of layer 1 and layer 2 (h_1 and h_2). Crosses denote the median of the PDM, while dots indicate the best-fitting model.

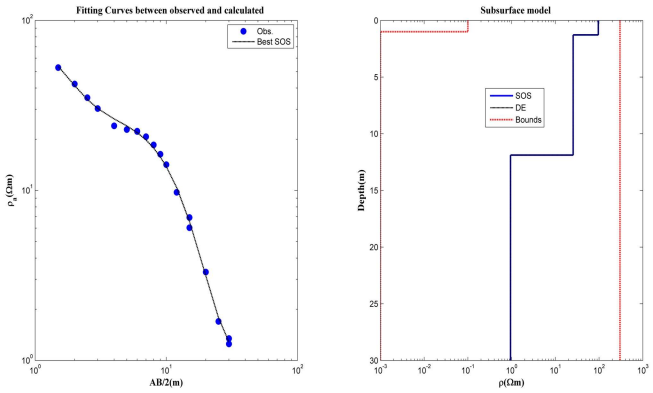

Figure 10 Inversion results of observed VES data, comparison between observed VES data dispersion (solid dots) and the best modeled VES data using IMSOS (solid lines) (left), the lower and upper bounds of the search area (dashed lines) and inverted resistivity profiles (solid line) using IMSOS and DE (right).

Table 4 Search space and inversions results and their uncertainties using IMSOS and DE for field VES data.

Parameters	Search Space	DE	IMSOS
h1 (m)	1 - 15	1.28±0.00	1.28±0.00
h2 (m)	1 - 20	10.60±0.00	10.60±0.00
ρ1 (Ωm)	0.1 - 300	96.05±0.05	96.05±0.04
ρ2 (Ωm)	0.001 - 300	25.50±0.00	25.50±0.00
ρ3 (Ωm)	0.0001 - 300	0.95±0.00	0.95±0.00

8 Conclusion

In this study, a new improved modified SOS algorithm (IMSOS) for solving geophysical inversion problems was presented. The parasitism phase of the original MSOS was modified and tested on the Ackley and the Griewank testing functions. Like the standard SOS and MSOS algorithms, IMSOS is also adaptive and tuning parameter free while having a good equilibrium between its exploration and exploitation capabilities, which is required for solving inversion problems in geophysics. The algorithm also has the capability of constructing a PDM from generated samples of the search space. In order to demonstrate its performance, the IMSOS algorithm was applied to noisy synthetic data sets of SP and VES data. Moreover, the algorithm was also used to invert an SP and VES field data set from the LUSI mudflow embankment, Sidoarjo, East Java, Indonesia. Other population-based algorithms, i.e. PSO, DE and BHA, were employed for comparison with the IMSOS algorithm.

The synthetic and field data inversions showed that the IMSOS algorithm is effective for geophysical data inversion, leading to good results and providing the uncertainty of the model parameters through a PDM from the inversion process. In addition, the inverse models resulting from IMSOS were comparable with the results from similar population or swarm-based algorithms. However, we found that the proposed algorithm still suffers from a fundamental limitation of the global approach of inverse problems, i.e. many evaluations need forward modeling, which hinders its use for very complex forward modeling algorithms with a large number of model parameters.

Acknowledgements

The authors would like to thank BPLS for permission to publish the data used in this paper. Hendra Grandis received an overseas research grant from the Asahi Glass Foundation in 2018, while Sungkono was supported by BRIN (Badan Riset dan Inovasi Nasional) with contract nr. 930/PKS/ITS/2021.

References

[1] Fernández-Martínez, J.L., Pallero, J.L.G., Fernández-Muñiz, Z. & Pedruelo-González, L.M., *The Effect of Noise and Tikhonov's Regularization in Inverse Problems. Part I: The Linear Case*, Journal of Applied Geophysics, **108**(9), pp. 176-185, 2014.

[2] Fernández-Muñiz, Z., Hassan, K. & Fernández-Martínez, J.L., *Data Kit Inversion and Uncertainty Analysis*, Journal of Applied Geophysics **161**(1), pp. 228-238, 2019.

[3] Sungkono & Santosa, B.J., *Differential Evolution Adaptive Metropolis Sampling Method to Provide Model Uncertainty and Model Selection Criteria to Determine Optimal Model for Rayleigh Wave Dispersion*, Arabian Journal of Geosciences, **8**(9), pp. 7003-7023, 2015.

[4] Tarantola, A., *Popper, Bayes and the Inverse Problem*, Nature Physics, **2**(8), pp. 492-494, 2006.

[5] Vrugt, J.A., *Markov Chain Monte Carlo Simulation Using the DREAM Software Package: Theory, Concepts, and MATLAB Implementation*, Environmental Modelling & Software, **75**(1), pp. 273-316, 2016.

[6] Fernández-Alvarez, J.P., Fernández Martínez, J.L. & Menéndez-Pérez, C.O., *Feasibility Analysis of the Use of Binary Genetic Algorithms as Importance Samplers Application to A 1-D DC Resistivity Inverse Problem*, Mathematical Geosciences, **40**(4), pp. 375-408, 2008.

[7] Fernández-Martínez, J.L., García Gonzalo, E., Fernández Álvarez, J.P., Kuzma, H.A. & Menéndez-Pérez, C.O., *PSO: A Powerful Algorithm to Solve Geophysical Inverse Problems: Application to a 1D-DC Resistivity Case*, Journal of Applied Geophysics, **71**(1), pp. 13-25, 2010.

[8] Balkaya, Ç., *An Implementation of Differential Evolution Algorithm for Inversion of Geoelectrical Data*, Journal of Applied Geophysics, **98**, pp. 160-175, 2013.

[9] Sungkono & Warnana, D.D., *Black Hole Algorithm for Determining Model Parameter in Self-Potential Data*, Journal of Applied Geophysics, **148**, pp. 189-200, 2018.

[10] Sungkono, *Robust Interpretation of Single and Multiple Self-Potential Anomalies via Flower Pollination Algorithm*, Arabian Journal of Geosciences, **13**(3), 2020.

[11] Hatamlou, A., *Black Hole: A New Heuristic Optimization Approach for Data Clustering*, Information Sciences, **222**, pp. 175-184, 2013.

[12] Cheng, M.Y. & Prayogo, D., *Symbiotic Organisms Search: A New Metaheuristic Optimization Algorithm*, Computers & Structures, **139**, pp. 98-112, 2014.

[13] Javidy, B., Hatamlou, A. & Mirjalili, S., *Ions Motion Algorithm for Solving Optimization Problems*, Applied Soft Computing, **32**, pp. 72-79, 2015.

[14] Mirjalili, S., *Dragonfly Algorithm: A New Meta-Heuristic Optimization Technique for Solving Single-Objective, Discrete, and Multi-Objective Problems*, Neural Computing & Applications, **27**, pp. 1053-1073, 2016.

[15] Zhang, J. & Sanderson, A.C., *JADE: Adaptive Differential Evolution with Optional External Archive*, IEEE Transactions on Evolutionary Computation, **13**(5), pp. 945-958, 2009.

[16] Faramarzi, A., Haidarinejad, M., Mirjalili, S. & Gandomi, A.H., *Marine Predators Algorithm: A Nature-Inspired Metaheuristic*, Expert Systems with Applications **152**, pp. 113377, 2020.

[17] Kumar, S., Tejani, G.G. & Mirjalili, S., *Modified Symbiotic Organisms Search for Structural Optimization*, Engineering with Computers, **35**, pp. 1269-1296, 2018.

[18] Tejani, G.G., Savsani, V.J. & Patel, V.K., *Adaptive Symbiotic Organisms Search (SOS) Algorithm for Structural Design Optimization*, Journal of Computational Design and Engineering, **3**(3), pp. 226-249, 2016.

[19] Das, S., Bhattacharya, A. & Chakraborty, A.K., *Solution of Short-Term Hydrothermal Scheduling Problem Using Quasi-Reflected Symbiotic Organisms Search Algorithm Considering Multi-Fuel Cost Characteristics of Thermal Generator*, Arabian Journal of Science and Engineering, **43**, pp. 2931-2960, 2018.

[20] Dib, N., *Design of Planar Concentric Circular Antenna Arrays with Reduced Side Lobe Level Using Symbiotic Organisms Search*, Neural Computing & Applications, **30**, pp. 3859-3868, 2018.

[21] Sharma, S.P., *VFSARES-A Very Fast Simulated Annealing FORTRAN Program for Interpretation of 1-D DC Resistivity Sounding Data from Various Electrode Arrays*, Computers & Geosciences, **42**, pp. 177-188, 2012.

[22] Ezugwu, A.E. & Prayogo, D., *Symbiotic Organisms Search Algorithm: Theory, Recent Advances and Applications*, Expert Systems with Applications, **119**, pp. 184-209, 2019.

[23] Prayogo, D., Cheng, M.Y., Wong, F.T., Tjandra, D. & Tran, D.H., *Optimization Model for Construction Project Resource Leveling Using a Novel Modified Symbiotic Organisms Search*, Asian Journal of Civil Engineering, **19**, pp. 625-638, 2018.

[24] Mehanee, S.A., *An Efficient Regularized Inversion Approach for Self-Potential Data Interpretation of Ore Exploration Using a Mix of Logarithmic and Non-Logarithmic Model Parameters*, Ore Geology Reviews, **57**, pp. 87-115, 2014.

[25] Monteiro-Santos, F.A., *Inversion of Self-Potential of Idealized Bodies' Anomalies Using Particle Swarm Optimization*, Computers & Geosciences, **36(**9), pp. 1185-1190, 2010.

[26] Ojo, A.O., Xie, J. & Olorunfemi, M.O., *Nonlinear Inversion of Resistivity Sounding Data for 1-D Earth Models Using the Neighbourhood Algorithm*, Journal of African Earth Sciences, **137**, pp. 179-192, 2018.

[27] Di Maio, R., Piegari, E., Rani, P., Carbonari, R., Vitagliano, E. & Milano, L., *Quantitative Interpretation of Multiple Self-Potential Anomaly Sources by A Global Optimization Approach*, Journal of Applied Geophysics, **162**, pp. 152-163, 2019.

[28] Biswas, A., *A Review On Modeling, Inversion and Interpretation of Self-Potential in Mineral Exploration and Tracing Paleo-Shear Zones*, Ore Geology Reviews, **91**, pp. 21-56, 2017.

[29] Abdelazeem, M., Gobashy, M., Khalil, M.H. & Abdrabou, M., *A Complete Model Parameter Optimization from Self-Potential Data Using Whale Algorithm*, Journal of Applied Geophysics, **170**, pp. 103825, 2019.

[30] Husein, A., Sungkono, Wijaya, A. & Hadi, S., *Subsurface Monitoring of P.79-P.82 LUSI Embankment Using GPR Method to Locate Subsidence and Possible Failure*, in 15th International Conference on Ground Penetrating Radar (GPR), Brussels, Belgium, pp. 268-273, 2014.

[31] Sungkono, Feriadi, Y., Husein, A., Prasetyo, H., Charis, M., Irawan, D., Rochman, J.P.G.N., Bahri, A.S. & Santosa, B.J., *Assessment of Sidoarjo Mud Flow Embankment Stability Using Very Low Frequency Electromagnetic Method*, Environmental Earth Sciences, **77**(5), pp. 196 ref. 81, 2018.

[32] Sungkono, Husein, A., Prasetyo, H., Bahri, A.S., Monteiro Santos, F.A. & Santosa, B.J., *The VLF-EM Imaging of Potential Collapse on the LUSI Embankment*, Journal of Applied Geophysics **109**, 218-232, 2014.

[33] Sungkono, Wasilah, M.N., Widyaningrum, Y., Hidayatullah, W.M., Fathoni, F.A. & Husein, A., *Self-Potential Method to Assess Embankment Stability: A Study Related to The Sidoarjo Mud Flow*, Journal of Engineering and Technological Sciences, **52**(5), pp. 707-731, 2020.